SYNTHESIS, CHARACTERIZATION AND X-RAY STUDIES OF SOME P, As AND Sb LIGANDS SUBSTITUTED CLUSTER COMPLEXES OF $Ru_3(CO)_{12}$

SITI SYAIDA BINTI SIRAT

UNIVERSITI SAINS MALAYSIA

2013

SYNTHESIS, CHARACTERIZATION AND X-RAY STUDIES OF SOME P, As AND Sb LIGANDS SUBSTITUTED CLUSTER COMPLEXES OF $Ru_3(CO)_{12}$

by

SITI SYAIDA BINTI SIRAT

Thesis submitted in fulfillment of the requirements

for the Degree of

Master of Science

July 2013

ACKNOWLEDGEMENT

First of all, I would like to sincerely thank my supervisor Prof Datuk Dr. Omar bin Shawkataly, for his encouragement, generosity, guidance, inspiration and support. I am also grateful to Dr. Imthyaz Ahmad Khan, Dr. Norlidah Al-Qadri and Dr. Abu Tariq Malick for advice and encouragement during the course of study. I wish to express my gratitude to USM for fellowship and Postgraduate Research Grant Scheme (PRGS).

I would like to express my sincere appreciation to all the staffs in the School of Distance Education and School of Chemical Sciences for providing me with facilities and assistances. I am thankful to the technical staffs of the School of Chemical Sciences, USM in particular Mr. Zahari Othman and Mr. Mohd Radzly. I would also like to thank the X-Ray Crystallography Unit of the School of Physics, USM.

I am deeply grateful to my colleagues for their help and moral support. I would like to thank my father, Sirat bin Rasip and my siblings for their constant support and encouragement. Finally, I am grateful to my mother, Che Tah binti Baharom for whom words cannot adequately express my gratitude.

TABLE OF CONTENTS

		Page
ACKNOWLEDGEMENT		ii
TABLE OF CONTENTS		iii
LIST OF TABLES		vi
LIST OF FIGURES		ix
SCHEME		xi
LIST OF ABBREVIATIONS		xii
ABSTRAK		xv
ABSTRACT		xvii
CHAPTER 1-INTRODUCTION		1
1.1	Metal cluster chemistry	1
1.2	Triruthenium dodecacarbonyl	2
1.3	Group 15 ligands	4
1.4	Objectives	7
1.5	Scope of the study	8
CHAPTER 2-LITERATURE REVIEW		9
2.1	Substitution chemistry of triruthenium cluster complexes with monodentate ligands	9
2.2	Substitution chemistry of triruthenium cluster complexes with bidentate ligands	20

2.3 Substitution chemistry of triruthenium cluster complexes with monodentate and bidentate ligands 28

CHAPTER 3-EXPERIMENTAL 34

3.1 Introduction 34

3.2 Synthesis of $Ru_3(CO)_{10}(LL)$ [LL=dppb and dpph] 36

3.3 Synthesis of $Ru_3(CO)_9(LL)As((C_6H_4)Ph)_3$ [LL=dppm and dpam] 38

3.4 Synthesis of $Ru_3(CO)_9(dppe)(L')$ [L'= $As(C_6H_4OMe\text{-}p)_3$ and $SbPh_3$] 39

3.5 Synthesis of $Ru_3(CO)_9(arphos)(L')$ [L'= PCy_3, PPh_3, $P(C_6H_4F\text{-}m)_3$, $P(C_6H_4F\text{-}p)_3$, $P(C_6H_4Cl\text{-}p)_3$, and $PPh(C_6H_4OMe\text{-}p)_2$] 40

3.6 Synthesis of $Ru_3(CO)_9(arphos)(L')$ [L'= $AsPh_3$, $As(C_6H_4Me\text{-}m)_3$ and $As(C_6H_4Me\text{-}p)_3$] 44

3.7 Synthesis of $Ru_3(CO)_9(dppb)(L')$ [L'= PPh_3 and $PPh(C_6H_4OMe\text{-}p)_2$] 46

CHAPTER 4-RESULTS AND DISCUSSIONS 48

4.1 Structures of $Ru_3(CO)_{10}(dppb)$ and $Ru_3(CO)_{10}(dpph)$ 48

4.2 Structures of $Ru_3(CO)_9(LL)As((C_6H_4)Ph)_3$ [LL= dppm and dpam] 57

4.3 Structures of $Ru_3(CO)_9(dppe)(L')$ [L'= $As(C_6H_4OMe\text{-}p)_3$ and $SbPh_3$] 66

4.4 Structures of $Ru_3(CO)_9(arphos)(L')$ [L'= PCy_3, PPh_3, $P(C_6H_4F\text{-}m)_3$, $P(C_6H_4F\text{-}p)_3$, $P(C_6H_4Cl\text{-}p)_3$ and $PPh(C_6H_4OMe\text{-}p)_2$] 76

4.5 Structures of $Ru_3(CO)_9(arphos)(L')$ [L'=$AsPh_3$, $As(C_6H_4Me\text{-}m)_3$ and $As(C_6H_4Me\text{-}p)_3$] 99

4.6 Structures of $Ru_3(CO)_9(dppb)(L')$ [L'= PPh_3 and $PPh(C_6H_4OMe\text{-}p)_2$] 112

CHAPTER 5-CONCLUSION 121

REFERENCES 123

LIST OF PUBLICATIONS ARISING FROM THIS RESEARCH BY THE AUTHOR 135

LIST OF CONFERENCES PRESENTATION BY THE AUTHOR 137

APPENDICES

LIST OF TABLES

		Page
Table 2.1	Bond lengths (Å) in $Ru_3(CO)_{11}(L)$ complexes	16
Table 2.2	Bond lengths (Å) in $Ru_3(CO)_{10}(L)_2$ complexes	18
Table 2.3	Bond lengths (Å) in $Ru_3(CO)_9(L)_3$ complexes	19
Table 2.4	Bond lengths (Å) in $Ru_3(CO)_{10}(LL)$ complexes	26
Table 2.5	Bond lengths (Å) in $Ru_3(CO)_9(LL)(L')$ complexes	31
Table 4.1	Crystal data and structure refinement for $Ru_3(CO)_{10}$(dppb) and $Ru_3(CO)_{10}$(dpph)	52
Table 4.2	Selected bond lengths and angles for $Ru_3(CO)_{10}$(dppb)	55
Table 4.3	Selected bond lengths and angles for $Ru_3(CO)_{10}$(dpph)	56
Table 4.4	Crystal data and structure refinement for Ru_3(dppm)As$((C_6H_4)Ph)_3$ and Ru_3(dpam)As$((C_6H_4)Ph)_3$	61
Table 4.5	Selected bond lengths and angles for Ru_3(dppm)As$((C_6H_4)Ph)_3$	64
Table 4.6	Selected bond lengths and angles for Ru_3(dpam)As$((C_6H_4)Ph)_3$	65
Table 4.7	Crystal data and structure refinement for $Ru_3(CO)_9$(dppe)As$(C_6H_4OMe\text{-}p)_3$ and $Ru_3(CO)_9$(dppe)$SbPh_3$	70
Table 4.8	Selected bond lengths and angles for $Ru_3(CO)_9$(dppe)As$(C_6H_4OMe\text{-}p)_3$	73
Table 4.9(a)	Selected bond lengths and angles for $Ru_3(CO)_9$(dppe)$SbPh_3$ Molecule A	74
Table 4.9(b)	Selcted bond lengths and angles for $Ru_3(CO)_9$(dppe)$SbPh_3$ Molecule B	75

Table 4.10	Crystal data and structure refinement for $Ru_3(CO)_9(arphos)PCy_3$ and $Ru_3(CO)_9(arphos)PPh_3$	83
Table 4.11	Selected bond lengths and angles for $Ru_3(CO)_9(arphos)PCy_3$	86
Table 4.12	Selected bond lengths and angles for $Ru_3(CO)_9(arphos)PPh_3$	87
Table 4.13	Crystal data and structure refinement for $Ru_3(CO)_9(arphos)P(C_6H_4F\text{-}m)_3$ and $Ru_3(CO)_9(arphos)P(C_6H_4F\text{-}p)_3$	88
Table 4.14	Selected bond lengths and angles for $Ru_3(CO)_9(arphos)P(C_6H_4F\text{-}m)_3$	91
Table 4.15	Selected bond lengths and angles for $Ru_3(CO)_9(arphos)P(C_6H_4F\text{-}p)_3$	92
Table 4.16	Crystal data and structure refinement for $Ru_3(CO)_9(arphos)P(C_6H_4Cl\text{-}p)_3$ and $Ru_3(CO)_9(arphos)PPh(C_6H_4OMe\text{-}p)_2$	93
Table 4.17	Selected bond lengths and angles for $Ru_3(CO)_9(arphos)P(C_6H_4Cl\text{-}p)_3$	96
Table 4.18	Selected bond lengths and angles for $Ru_3(CO)_9(arphos)PPh(C_6H_4OMe\text{-}p)_2$	97
Table 4.19	Comparison of selected bond lengths for $Ru_3(CO)_9(arphos)(L')$ [L'=PCy_3, PPh_3, $P(C_6H_4F\text{-}m)_3$, $P(C_6H_4F\text{-}p)_3$, $P(C_6H_4Cl\text{-}p)_3$, and $PPh(C_6H_4OMe\text{-}p)_2$	98
Table 4.20	Crystal data and structure refinement for $Ru_3(CO)_9(arphos)AsPh_3$	103
Table 4.21	Selected bond lengths and angles for $Ru_3(CO)_9(arphos)AsPh_3$	105
Table 4.22	Crystal data and structure refinement for $Ru_3(CO)_9(arphos)As(C_6H_4Me\text{-}m)_3$ and $Ru_3(CO)_9(arphos)As(C_6H_4Me\text{-}p)_3$	106

Table 4.23	Selected bond lengths and angles for $Ru_3(CO)_9$(arphos)As(C_6H_4Me-*m*)$_3$	109
Table 4.24(a)	Selected bond lengths and angles for $Ru_3(CO)_9$(arphos)As(C_6H_4Me-*p*)$_3$ Molecule A	110
Table 4.24(b)	Selected bond lengths and angles for $Ru_3(CO)_9$(arphos)As(C_6H_4Me-*p*)$_3$ Molecule B	111
Table 4.25	Crystal data and structure refinement for $Ru_3(CO)_9$(dppb)PPh_3 and $Ru_3(CO)_9$(dppb)PPh(C_6H_4OMe-*p*)$_2$	116
Table 4.26	Selected bond lengths and angles for $Ru_3(CO)_9$(dppb)PPh_3	119
Table 4.27	Selected bond lengths and angles for $Ru_3(CO)_9$(dppb)PPh(C_6H_4OMe-*p*)$_2$	120

LIST OF FIGURES

		Page
Figure 2.1	Substituted triruthenium clusters by monodentate ligand $Ru_3(CO)_{12-n}L_n$ (n =1,2 ,3 and 4)	10
Figure 2.2	Structure diagrams of monosubstituted complexes by monodentate ligand	16
Figure 2.3	Structure diagrams of disubstituted complexes by monodentate ligand	18
Figure 2.4	Structure diagrams of trisubstituted complexes by monodentate ligand	19
Figure 2.5	General reaction structures of bidentate ligand with triruthenium cluster	21
Figure 2.6	Structure diagrams of disubstituted complexes by bidentate ligand	26
Figure 2.7	Structure diagrams of trisubstituted complexes by monodentate and bidentate ligands	31
Figure 4.1	The ORTEP diagram of $Ru_3(CO)_{10}$(dppb) with 50% probability of ellipsoids for non H-atoms	53
Figure 4.2	The ORTEP diagram of $Ru_3(CO)_{10}$(dpph) with 50% probability of ellipsoids for non H-atoms	54
Figure 4.3	The ORTEP diagram of Ru_3(dppm)As($(C_6H_4)Ph)_3$ with 50% probability of ellipsoids for non H-atoms	62
Figure 4.4	The ORTEP diagram of Ru_3(dpam)As($(C_6H_4)Ph)_3$ with 50% probability of ellipsoids for non H-atoms	63
Figure 4.5	The ORTEP diagram of $Ru_3(CO)_9$(dppe)As(C_6H_4OMe-$p)_3$ with 50% probability of ellipsoids for non H-atoms	71
Figure 4.6	The ORTEP diagram of $Ru_3(CO)_9$(dppe)$SbPh_3$ Molecule A with 50% probability of ellipsoids for non H-atoms	72

Figure 4.7	The ORTEP diagram of $Ru_3(CO)_9$(arphos)PCy_3 with 50% probability of ellipsoids for non H-atoms	84
Figure 4.8	The ORTEP diagram $Ru_3(CO)_9$(arphos)PPh_3 with 50% probability of ellipsoids for non H-atoms	85
Figure 4.9	The ORTEP diagram of $Ru_3(CO)_9$(arphos)$P(C_6H_4F\text{-}m)_3$ with 50% probability of ellipsoids for non H-atoms	89
Figure 4.10	The ORTEP diagram of $Ru_3(CO)_9$(arphos)$P(C_6H_4F\text{-}p)_3$ with 50% probability of ellipsoids for non H-atoms	90
Figure 4.11	The ORTEP diagram of $Ru_3(CO)_9$(arphos)$P(C_6H_4Cl\text{-}p)_3$ with 50% probability of ellipsoids for non H-atoms	94
Figure 4.12	The ORTEP diagram of $Ru_3(CO)_9$(arphos)$PPh(C_6H_4OMe\text{-}p)_2$ with 50% probability of ellipsoids for non H-atoms	95
Figure 4.13	The ORTEP diagram of $Ru_3(CO)_9$(arphos)$AsPh_3$ with 50% probability of ellipsoids for non H-atoms	104
Figure 4.14	The ORTEP diagram of $Ru_3(CO)_9$(arphos)$As(C_6H_4Me\text{-}m)_3$ with 50% probability of ellipsoids for non H-atoms	107
Figure 4.15	The ORTEP diagram of $Ru_3(CO)_9$(arphos)$As(C_6H_4Me\text{-}p)_3$ with 50% probability of ellipsoids for non H-atoms	108
Figure 4.16	The ORTEP diagram of $Ru_3(CO)_9$(dppb)PPh_3 with 50% probability of ellipsoids for non H-atoms	117
Figure 4.17	The ORTEP diagram of $Ru_3(CO)_9$(dppb)$PPh(C_6H_4OMe\text{-}p)_2$ with 50% probability of ellipsoids for non H-atoms	118

SCHEME

		Page
Scheme 2.1	Catalytic cycle of benzophenone ketyl radical anion reaction mechanism	12

LIST OF ABBREVIATIONS

Å	angstrom
Anal	analytical
arphos	1,2-bis(diphenylphosphinodiphenylarsino)ethane
As	arsenic
ax	axial
bma	2,3-bis(diphenylphosphino)maleic anhydride
˚C	degree Celcius
Calc	calculation
diop	4,5-bis(diphenylphosphinomethyl)-2,2-dimethyl-1,3-dioxolane
dcpm	bis(dicyclohexylphosphino)methane
dpam	bis(diphenylarsino)methane
dpbm	1,3-diphenyl-2,3-dihydro-1H-1,3-benzodiphosphine
dppa	bis(diphenylphosphino)amine
dpmb	1,2-bis(diphenylphosphinomethyl)benzene
dpae	1,2-bis(diphenylarsino)ethane
dppb	1,4-bis(diphenylphosphino)butane
dppbz	1,4-bis(diphenylphosphino)benzene
dppm	bis(diphenylphosphino)methane
dppe	1,2-bis(diphenylphosphino)ethane
dppee	bis(diphenylphosphino)ethylene
dppf	1,1’-bis(diphenylphosphino)ferrocene

dmpm	bis(dimetyhlphosphino)methane
Et	ethyl
eq	equatorial
F-dppe	bis(perfluoro-diphenylphosphino)ethane
ffars	tetrafluorocyclobutene-bis(dimethylarsine)
ffos	tetrafluorocyclobutene-bis(diphenylphosphine)
$f_6$fos	hexafluorocyclohexene-bis(diphenylphosphine)
g	gram
h	hour
Hz	hertz
IR	infrared
mapm	bis(di(*o*-*N*-methylanilinyl)phosphino)methane
Me	methyl
mg	milligram
min	minutes
ml	milliliter
mmol	millimoles
m.p.	melting point
MHz	megahertz
nap	1-naphthyl
NMR	nuclear magnetic resonance
ORTEP	Oak Ridge Thermal Ellipsoid Plot
P	phosphorus

Ph	phenyl
ppm	part per million
Pr^i	iso-propyl
PTA	1,3,5-triaza-7-phosphaadamantane
R	alkyl
R_f	retention factor
SADABS	Siemens Area Detector Absorption Correction
SAINT	Siemens Analytical X-ray Area-detector Integration
sec	seconds
THF	tetrahydrofuran
TLC	thin layer chromatography
TMS	tetramethylsilane

SINTESIS, PENCIRIAN DAN KAJIAN KRISTALOGRAFI SINAR-X GUGUSAN KOMPLEKS $Ru_3(CO)_{12}$ PENUKARGANTIAN LIGAN P, As DAN Sb

ABSTRAK

Gugusan triruthenium dengan penukargantian ligan Kumpulan 15 telah disintesis menggunakan kaedah terma dan natrium benzophenone ketil radikal anion. Struktur gugusan yang terhasil dicirikan menggunakan analisis unsur dan kaedah spektroskopi yang merangkumi IR, ^{1}H, ^{13}C dan ^{31}P NMR. Struktur molekul gugusan triruthenium ditentukan menggunakan pembelauan sinar-X. Dua daripada tujuh belas kompleks baru telah dikenal pasti yang terdiri daripada jenis struktur $Ru_3(CO)_{10}(LL)$ [di mana LL= ligan bidentat] dan selebihnya berstruktur $Ru_3(CO)_9(LL)(L')$ [di mana LL= ligan bidentat, L' = ligan monodentat]. Gugusan triruthenium dengan bis penukargantian adalah $Ru_3(CO)_{10}$(dppb) dan $Ru_3(CO)_{10}$(dpph). Ligan dppb dan dpph berada pada kedudukan ekuatorial dan ikatan Ru-Ru terpanjang untuk kedua-dua gugusan adalah ikatan Ru-Ru yang dihubung oleh ligan bidentat. Gugusan baru triruthenium dengan tris penukargantian adalah $Ru_3(CO)_9(LL)As((C_6H_4)Ph)_3$ [LL =dppm, dpam], $Ru_3(CO)_9$(dppe)(L') [L' = $As(C_6H_4OMe\text{-}p)_3$, $SbPh_3$], $Ru_3(CO)_9$(arphos)(L') [L'= PCy_3, PPh_3, $P(C_6H_4F\text{-}m)_3$, $P(C_6H_4F\text{-}p)_3$, $P(C_6H_4Cl\text{-}p)_3$, $PPh(C_6H_4OMe\text{-}p)_2$, $AsPh_3$, $As(C_6H_4Me\text{-}m)_3$, $As(C_6H_4Me\text{-}p)_3$], $Ru_3(CO)_9$(dppb)(L') [L'= PPh_3, $PPh(C_6H_4OMe\text{-}p)_2$]. Kesemua gugusan tris penukargantian menunjukkan panjang ikatan Ru-Ru terpanjang adalah ikatan yang berkedudukan *cis* kepada ligan monodentat kecuali gugusan $Ru_3(CO)_9$(arphos)PPh_3, $Ru_3(CO)_9$(arphos)$AsPh_3$ dan

$Ru_3(CO)_9(dppb)PPh_3$ di mana ikatan Ru-Ru terpanjang adalah ikatan yang dihubungkan oleh ligan bidentat. Bagi kesemua gugusan, ligan bidentat dan monodentat Kumpulan 15 didapati berkedudukan ekuatorial.

SYNTHESIS, CHARACTERIZATION AND X-RAY STUDIES OF SOME P, As AND Sb LIGANDS SUBSTITUTED CLUSTER COMPLEXES OF $Ru_3(CO)_{12}$

ABSTRACT

Triruthenium cluster substituted with Group 15 ligands were synthesized by using sodium benzophenone ketyl radical anion and thermal method. The structures of the resulting clusters were elucidated by means of elemental analysis and spectroscopic methods, such as IR, ^{1}H, ^{13}C and ^{31}P NMR spectroscopy. The molecular structures of the resulting clusters were determined by X-ray diffraction. Two out of the seventeen new complexes thus identified consist of the type $Ru_3(CO)_{10}(LL)$ [where LL = bidentate ligand] and the other complexes of the type $Ru_3(CO)_9(LL)(L')$ [where LL= bidentate ligand, L'= monodentate ligand]. The disubstituted triruthenium clusters are $Ru_3(CO)_{10}$(dppb) and $Ru_3(CO)_{10}$(dpph). Both of the dppb and dpph ligands were occupying equatorial positions and the longest Ru-Ru bonds for both clusters belong to Ru-Ru bond that bridged by bidentate diphosphine ligand. The new trisubstituted triruthenium clusters are $Ru_3(CO)_9(LL)As((C_6H_4)Ph)_3$ [LL = dppm, dpam], $Ru_3(CO)_9$(dppe)(L') [L' = $As(C_6H_4OMe\text{-}p)_3$, $SbPh_3$], $Ru_3(CO)_9$(arphos)(L') [L'= PCy_3, PPh_3, $P(C_6H_4F\text{-}m)_3$, $P(C_6H_4F\text{-}p)_3$, $P(C_6H_4Cl\text{-}p)_3$, $PPh(C_6H_4OMe\text{-}p)_2$, $AsPh_3$, $As(C_6H_4Me\text{-}m)_3$, $As(C_6H_4Me\text{-}p)_3$], $Ru_3(CO)_9$(dppb)(L') [L' =PPh_3, $PPh(C_6H_4OMe\text{-}p)_2$]. All trisubstituted clusters show that the longest Ru-Ru bonds are the bonds *cis* to the monodentate ligand with exception for the clusters of $Ru_3(CO)_9$(arphos)PPh_3, $Ru_3(CO)_9$(arphos)$AsPh_3$ and $Ru_3(CO)_9$(dppb)PPh_3, which show the bidentate ligand

bridges longest Ru-Ru bond. For all the clusters, Group 15 monodentate and bidentate ligands, all are found to occupy equatorial positions.

CHAPTER 1

INTRODUCTION

1.1 Metal cluster chemistry

Interest in the chemistry of transition metal clusters started about 60 years ago. This area of chemistry lies at the interface between conventional organic and inorganic chemistry as it involves the interaction between inorganic metal ions and organic molecules or organic functional groups. Metal cluster complexes are defined as compounds with three or more metal atoms connected to each other by direct metal-metal bonding [1].

Many cluster molecules are constructed from transition metal atoms which are coordinated to π-acid ligands, in particular ligands such as carbon monoxide, cyclopentadienyl and phosphines. The π-acceptor or π-acid ligands help to produce the most constructive condition for metal-metal bond formation of the Group 8-10 elements by inducing the greatest overlap between the atomic orbitals of the metal. The formation of metal-metal bonds is important to construct cluster complexes. The bonding between metal and carbon monoxide always involves coordination of the carbon atom through donation of the lone pair of electrons on the carbon atom to an empty metal d orbital of σ symmetry and back donation from filled metal d orbitals to the empty π* C-O antibonding orbital [2].

The metal cluster provides a framework in which ligands are able to coordinate to one or more metal centres [1]. Type of ligands can also influence the nuclearity and geometry of the cluster by exerting its steric effect. For example, as

the ligand size increases, the rates of reactions leading to metal-metal bond formation are reduced and for a given ligand/metal ratio, the higher-nuclearity clusters are destabilized by ligand-ligand repulsion effects [3].

Increasing interest in the study of the metal clusters are mainly due to the fact that metal clusters can act as effective homogenous catalysts [4-5]. The properties of metal cluster that are built from three or more metal centre help to facilitate activation and transformation of the substrates, and high mobility of the ligands could promote reactions between several molecules bonded to the cluster framework [2]. Metal cluster complexes had played a very important role in many chemical reactions, for example act as catalysts for carbonylation of alcohols [6-7], isomerization and hydrogenation of olefins [7-10], water gas shift reaction [11] and hydroformylation of alkenes [12].

In addition, cluster compounds are generally labile and their reactivities are high. Hence, these cluster compounds may be exploited by taking advantage of their high reactivity. Moreover, transition metal complexes and clusters have a high coordination affinity for a variety of monodentate, bidentate and polydentate ligands. It is crucial for synthetic chemists to understand the underlying reactions in the coordination sphere of metal atoms, which are fundamental metal transformations and substitutions of ligands that modify the metal fragments.

1.2 Triruthenium dodecacarbonyl

One of the most studied metal carbonyl cluster that attracts researcher's attention is triruthenium dodecacarbonyl, $Ru_3(CO)_{12}$. The first ruthenium carbonyl

was discovered in 1910 by Mond and co-workers, who isolated an unidentified volatile orange solid from reaction of ruthenium metal with carbon monoxide at 300˚C and 400 atmosphere pressure. The product obtained as a ruthenium carbonyl, but it was not correctly characterized [13]. Then, Corey and Dahl in 1961 [14] characterized and formulated it as $Ru_3(CO)_{12}$ on the basis of X-ray crystallography of the osmium analogue. In 1966, Bruce and Stone published an improved synthesis of $Ru_3(CO)_{12}$ by carbonylation (<10 atm., 65˚C) of ruthenium trichloride in methanol in the presence of suitable halogen acceptor [15]. Later in 1983, Bruce and co-workers reported the best preparation of $Ru_3(CO)_{12}$ by the carbonylation of a 1% methanol solution of hydrated ruthenium trichloride at 50-60 atmosphere pressure and 125 ˚C [16].

The early crystal structure of $Ru_3(CO)_{12}$ established by X-ray diffraction have shown that all twelve carbonyls are being terminally bonded in axial and equatorial positions with the crystal system being monoclinic. These relatively low precision structure and the reported Ru-CO bond lengths are such that average Ru-CO (axial) distance of 1.89 (2) Å is slightly shorter than the average Ru-CO (equatorial) distance of 1.93 Å [17]. Later, Churchill and co-workers reported an accurate redetermination of the structure of $Ru_3(CO)_{12}$ with the conclusion that the axial Ru-CO bond lengths are longer than the equatorial Ru-CO linkages. This was done by showing the average of axial Ru-CO bond lengths to be 1.942 (4) Å while equatorial Ru-CO shows 1.921 (5) Å [18]. In addition, it was reported that crystal structure of $Ru_3(CO)_{12}$ have no disorder compared to $Fe_3(CO)_{12}$ where two carbonyl groups bridging one of the Fe-Fe triangle edges and the other ten carbonyls are in terminal positions. Disorder in $Fe_3(CO)_{12}$ arises because the molecule is located around an

inversion centre which results from the space average of molecules in two centre symmetric orientations [19].

The basic building block in $Ru_3(CO)_{12}$ cluster is the three Ru metal atoms. This metal cluster triangle can be used to construct metal cluster of higher nuclearity. Metal triangles can be joined by sharing edges or vertices to form more complicated metal cluster networks [20] and can be stacked either directly on top of each other or with other metal atoms between pairs of triangles [21]. Moreover, different types of ligands have the potential to coordinate or substitute with these transition metal carbonyl clusters, depending on the coordination reactivity of these ancillary ligands based on their stability and reactivity of the associated metals [2]. These contribute to an idea of substituting different ligand with variety of chemical and physical properties to transition metal carbonyl clusters. Knowledge of the chemical and physical properties of these new clusters will help to develop a clearer understanding of surface phenomena relating to their applications.

1.3 Group 15 ligands

A ligand is defined as a molecule or anion bonded to the central metal atom to form a metal complex [22]. The bonding between metal and ligand generally involves formal donation of one or more of the ligand's electron pairs and display a wide range of steric and electronic effects upon complexation with metal centres. Ligand can be classified as monodentate, bidentate or polydentate. Group 15 ligands are effective ligands to coordinate with transition metal. A large number of metal complex containing Group 15 ligand atoms have been reported due to versatility of their electronic and steric properties as well as their numerous applications [23-24].

The Group 15 ligands consisting of P, As and Sb elements had prompted researchers to study their special properties in such a way to come out with such new complexes that contribute to new fundamental knowledge and its application. The steric and electronic properties of the ligand which can be altered in a periodic and systematic fashion by varying the nature of the R- group attached to the Group 15 atom [25-26]. This makes these Group 15 monodentate ligands to form stabilized cluster complexes. The steric bulk of a phosphine ligand was determined from the size of ligand cone angle to indicate the approximate space occupied by the ligand about the metal centre [27]. Indeed, tertiary phosphine ligands are capable enough to coordinate with the transition metal complexes because of their high affinity for the metal [28].

The fascinating derivative chemistry of metal cluster with Group 15 monodentate ligands that adopted simple terminal [29-30], edge-bridged [31-32] and face-capped [33-34] have been widely reported. Thus, metal cluster complexes containing these ligands become more exciting and challenging in the research of new catalytic systems for the development of new, diverse and stable metal cluster complexes that will influence the reaction efficiency in terms of catalytic activity.

Another important type of Group 15 ligand is bidentate phosphine or arsine that contains a carbon backbone linking the Group 15 element. For example, the most common bidentate phosphine ligands are of the type $PPh_2(CH_2)nPPh_2$, where n= 1-6 have been widely used in organometallic reactions over the years [35-39]. In addition, bidentate ligand can also possess two different Group 15 donor atoms and are known as mixed bidentate ligand. For example, the arphos ligand with chemical formula, $Ph_2PCH_2CH_2AsPh_2$, is a mixed bidentate ligand with As and P atoms linked by two methylene carbon backbone [40].

Bidentate ligands can play a major role in stabilizing metal cluster by coordinating in different modes. The bidentate ligand has been found to adopt a variety of bonding modes on the cluster, including monodentate, chelating a single metal atom in the cluster, bridging across a metal-metal bond and forming an intermolecular link across two clusters. Reactions conducted by Bruce and co-workers in 1982 which deal with $Ru_3(CO)_{12}$ and bis(diphenylphosphino)ethane (dppe) has been reported to function as a monodentate, bidentate and chelating ligand [36]. In addition, they also serve as a bridging ligand cross a metal-metal bond, and as a connecting ligand in the complex $[Ru_3(CO)_{11}]_2$dppe, whereby two metal cluster units are connected through ditertiary-phosphine ligands [36].

Particularly, diphoshine such as dppm and dppe are important subclass of tertiary phosphines with widespread use in homogeneous catalysis. A key to their success in this area is their ability to tune their spatial demands by variation of substituents at phosphorus and also the nature of the adjoining backbone [41]. Indeed, their bridging versus chelating behavior is still a matter of interest. For example, diphosphine ligands in turn are able to confer extra stability to their complexes as a result of their ability to bridge metal centres [27, 42-43]. The bite angle has an influence on the metal-metal separation [44]. Indeed, the steric properties of diphosphine ligand are determined by the four substituents at the two phosphorus atoms and the length of carbon chain [41, 45]. Thus, studies involving the reaction of metal clusters with different Group 15 ligands have led to a better understanding of the factors that responsible for metal skeletal transformations.

The design, synthesis and characterization of metal cluster complexes are essential in providing a suitable array of cluster that contains the necessary stoichiometry and bonding that required for the understanding of electronic influence

as well as the effect of the different ligands in the chemical behaviour of their cluster complexes. Nevertheless, metal cluster complexes have also been shown to be important in industry as homogeneous catalysts [4-5] and as precursors to bi- and trimetallic nanoparticle catalysts in heterogeneous catalysis [46-47], detailed knowledge of the bonding and geometry structure of these clusters are efforts that needed in providing a route from fundamental to applied science in this area of study. The research about synthesis, characterization and molecular structure which are results from the substitution of CO with dissimilar phosphine and arsine ligands are vital to understand the electronic and steric effects of the new cluster complexes.

1.4 Objectives

The objectives of this study are:

1. To synthesize new complexes of triruthenium cluster containing Group 15 monodentate and bidentate ligands
2. To characterize all new compounds through various analytical methods including infrared spectroscopy (IR), nuclear magnetic resonance (NMR), CHN analysis, X-ray diffraction(XRD)
3. To determine the molecular structures of new metal cluster complexes

1.5 Scope of the study

The research study on the synthesis of new compound by substituting carbonyl ligand in $Ru_3(CO)_{12}$ with Group 15 ligands be divided into two parts. The first part includes synthesizing six types of parent compounds of the type $Ru_3(CO)_{10}(LL)$ [where LL= $Ph_2PCH_2PPh_2$ (dppm), $Ph_2AsCH_2AsPh_2$ (dpam), $Ph_2P(CH_2)_2PPh_2$ (dppe), $Ph_2P(CH_2)_2AsPh_2$ (arphos), $Ph_2P(CH_2)_4PPh_2$ (dppb) and $Ph_2P(CH_2)_6PPh_2$ (dpph)]. The second part of the study was the substitution of another carbonyl of the parent compounds $Ru_3(CO)_{10}(LL)$ to produce organometallic cluster complexes of the type $Ru_3(CO)_9(LL)(L')$, where L' is Group 15 monodentate ligands.

All the new synthesized cluster complexes were characterized using infrared spectroscopy (IR), nuclear magnetic resonance (NMR), CHN analysis and single crystal X-ray diffraction (XRD). IR is one of the first spectroscopic techniques to be applied to the study of carbonyl clusters with its capability in identifying carbonyl stretching and other functional groups. CHN analysis is to determine the exact composition of organic element within the compound and NMR for determining the chemical shift of ^{1}H, ^{13}C and ^{31}P nuclei in the cluster complexes. A single crystal X-ray diffraction (XRD) study is required to obtain more detailed and accurate information about the atomic structure and geometric parameters. It is clear that these studies enable us to make a detailed comparison on the molecular geometries which results from the substitution of CO by Group 15 ligands. Besides, it is also enables the exploration of chemical properties of the novel cluster complexes. Moreover, the effort required to establish such novel cluster complexes will be rewarded with new opportunities in both fundamental science and its application.

CHAPTER 2

LITERATURE REVIEW

2.1 Substitution chemistry of triruthenium cluster complexes with monodentate ligands

The substitution chemistry of carbonyls (CO) in triruthenium cluster with Group 15 monodentate ligands has been extensively studied over the years with respect to the coordination mode adopted by the Group 15 ligands relative to the Ru_3 polyhedron. The reactions of $Ru_3(CO)_{12}$ with monodentate ligands in a different mole ratio will afford mono-, di-, tri- and tetrasubstituted when the $Ru_3(CO)_{12}$ was activated through various methods [30, 48-49]. The different degrees of substitution of Group 15 monodentate ligands are shown in Figure 2.1.

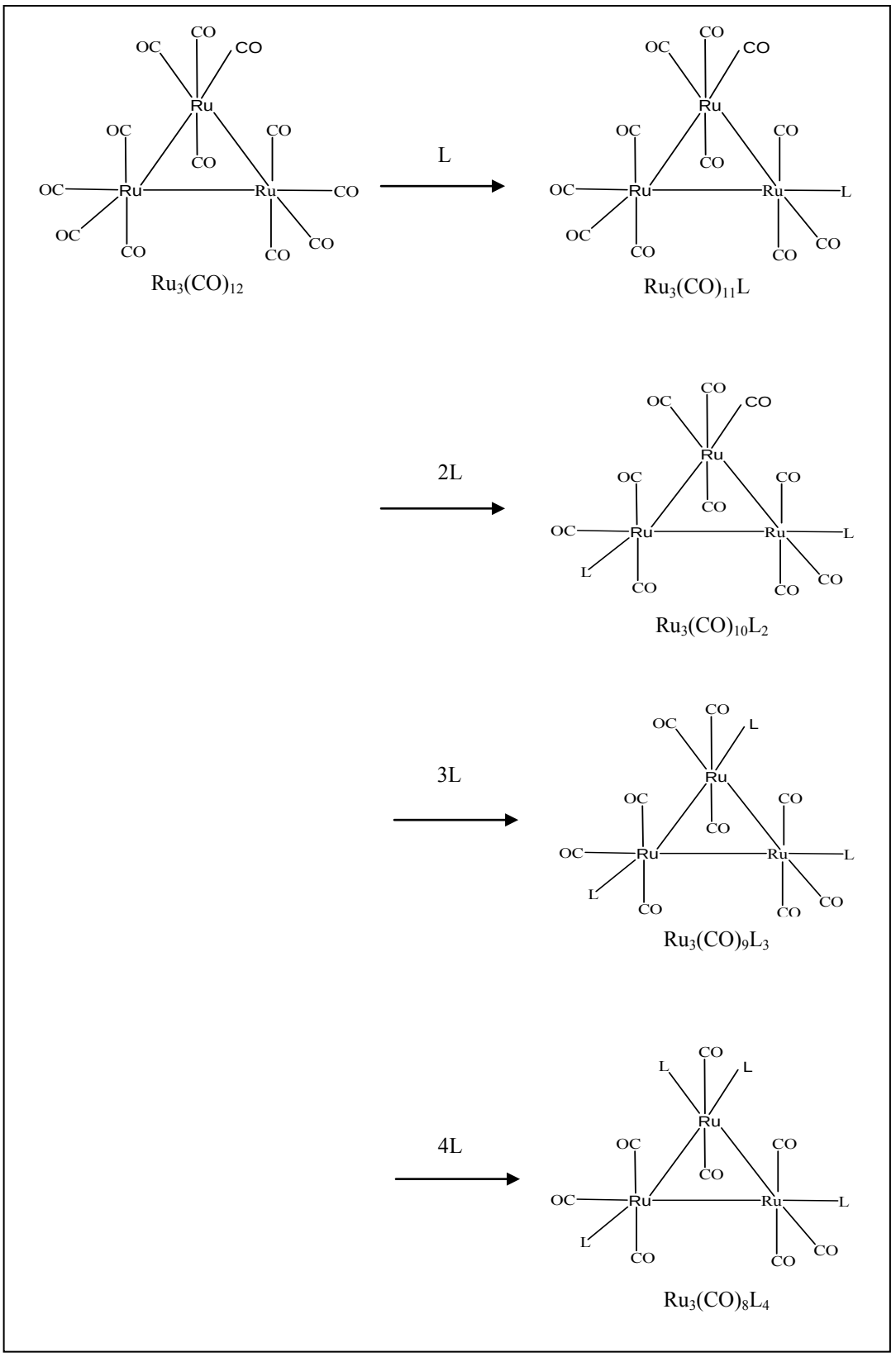

Figure 2.1 Substituted triruthenium clusters by monodentate ligand $Ru_3(CO)_{12-n}L_n$ (n =1,2,3 and 4)

The initial studies on $Ru_3(CO)_{12}$ substituted by PPh_3 afforded $Ru_3(CO)_9(PPh_3)_3$ using thermal reaction and was first reported in 1966 [50]. Before 1972, there was no mono or disubstituted complex of $Ru_3(CO)_{12}$ isolated due to the kinetic instability relative to the trisubstituted species [51].

In order to better understand the reactivity of that substituted triruthenium cluster with Group 15 ligands, Bruce and co-workers had introduced new methods to activate $Ru_3(CO)_{12}$. This was done by using sodium benzophenone ketyl radical anion to induce specific carbonyl substitution of the metal clusters. The addition of catalytic amounts of the sodium benzophenone ketyl radical anion solution to the metal cluster, along with appropriate stoichiometric amounts of phosphines affords the mono-, di-, tri- and tetrasubstituted cluster compounds and the reactions were completed within five minutes at room temperature [52]. This substitution involves an electron transfer catalysed (ETC) process. The proposed mechanism for the electron transfer process with $Ru_3(CO)_{12}$ is outlined in Scheme 2.1.

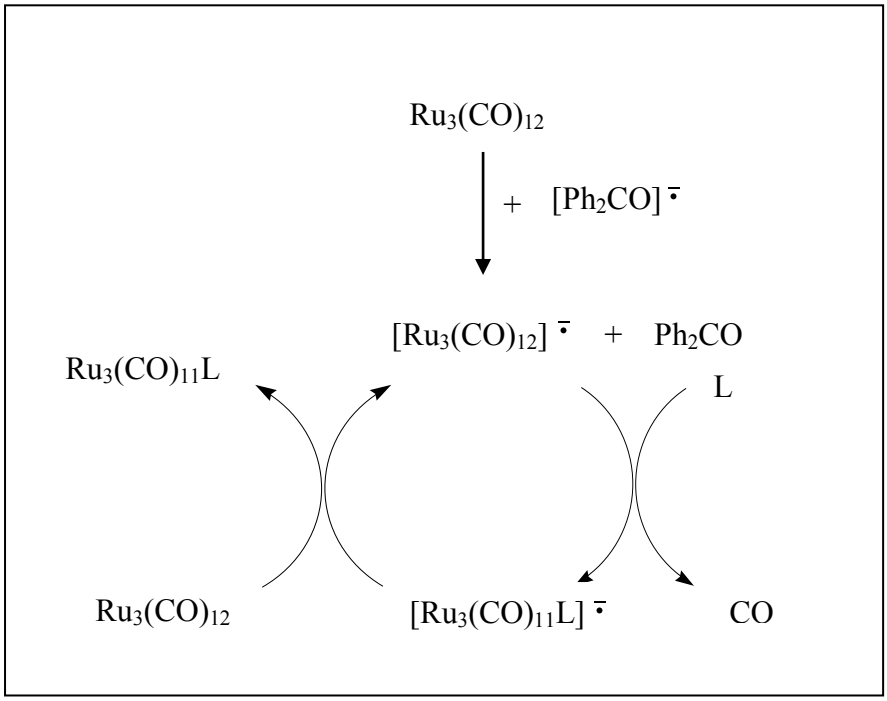

Scheme 2.1 Catalytic cycle of benzophenone ketyl radical anion reaction mechanism [52]

The radical anion $[Ru_3(CO)_{12}]^{\bullet-}$ becomes a reactive species where the extra electron is in antibonding orbital, leading to a weakened Ru-Ru metal bond. This bond cleaves, leaving a 17 electron centre, which will be attacked by phosphine resulting in the elimination of CO. The reformation of the metal-metal bond yields a substituted radical anion $[Ru_3(CO)_{11}L]^{\bullet-}$, which transfers an electron to an unsubstituted ruthenium cluster to continue the catalytic cycle [52].

The requirements for this reaction to occur are the cluster carbonyl needed to be reduced without fragmentation and the resulting radical has to have a long enough lifetime to allow for substitution. In order to facilitate the transfer of an electron from the substituted to unsubstituted radical anion, the substituting ligand must be a better Lewis base than the carbonyl ligand. Secondly, the ligand must not be reduced by the diphenylketyl radical anion. When these conditions are met, this method allows for

short reaction times, mild conditions, high product yields and also leads to the isolation of many complexes which were previously difficult to obtain. These techniques provide a convenient platform for preparation of a variety of substitution products. For example, the utility of this technique was shown in synthesizing of some mono, di- and tri-substituted cluster complexes of $Ru_3(CO)_{12}$ substituted by bulky fluorinated phosphine ligands; $Ru_3(CO)_{11}P(C_6H_4F\text{-}m)_3$, $Ru_3(CO)_{10}(P(C_6H_4F\text{-}p)_3)_2$, and $Ru_3(CO)_9(P(C_6H_4F\text{-}m)_3)_3$ [53]. Indeed, $Ru_3(CO)_{11}P(Cy)_3$, $Ru_3(CO)_{10}[P(OMe)_3]_2$, and $Ru_3(CO)_9[P(Me)_3]_3$ were also synthesized by this method [54]. In fact, the first example of reactions of metal carbonyls catalysed by anionic species was the specific formation of $Fe(CO)_4(L)$ (L=PPh_3, $P(OMe)_3$ or $P(OPh)_3$) from $Fe(CO)_5$ and L [55].

Another method of activating $Ru_3(CO)_{12}$ towards specific CO substitution also can be achieved by using [PPN][OAc] or [PPN][CN]. Lavinge and Kaesz discovered that with the use of a catalytic amount of [PPN][OAc] in the reaction would promoted substitution by tertiary phosphine such as PPh_3, dppm and dppe [56]. Subsequently, other $[PPN]^+$ salts show varying degrees of activity; rates of ligand substitution in $Ru_3(CO)_{12}$ enhanced by addition of methoxide ion, which formed the labile methoxycarbonyl complex $[Ru_3(CO_2Me)(CO)_{11}]^-$ [57-58]. These methods reveal that such complexes have a higher reactivity towards nucleophilic reagents, undergoing carbonyl substitution reactions and nucleophilic additions to coordinated CO ligands under very mild conditions [59]. Besides, Bruce and his research team have reported an interesting and well-documented study on series of stereochemistry of Group 15 ligands substituted derivatives of $Ru_3(CO)_{12}$ [60-62].

The complexes obtained were of the type $Ru_3(CO)_{12-n}(L)_n$, where [L= $PPh(OMe)_2$, n = 1, 2, 3 [60-62]; L= $P(OCH_2CF_3)_3$, n = 1,2,3 [60-62]; L = $AsMe_2Ph$, n = 3 [62]; L= PMe_2Ph , $P(OR)_3$, (R= Me, Et and Ph), n = 4] [63].

The structure of $Ru_3(CO)_8[PPh(OMe)_2]_4$, is the first ruthenium complex to have the $Fe_3(CO)_{12}$ structure with two CO ligands bridging one of the three Ru-Ru bonds [64]. Generally, the Group 15 ligands in the resulting product exclusively occupy an equatorial coordination site as expected on steric grounds. In contrast, the situation found for $Ru_3(CO)_{11}(CNBu^t)$ and $Ru_3(CO)_{10}(CNBu^t)_2$ [16] which occupy axial position.

In another important observation by Shawkataly and co-workers, the reaction between $Ru_3(CO)_{12}$ and $SbPh_3$ in THF and iniatiated by the sodium benzophenone ketyl anion radical, resulted in formation of $Ru_3(CO)_{10}[(C_6H_5)SbRu_3CO(C_6H_5)(CO)_{10}]$ which is an example of a bridged acylcarbonyl cluster. At first, the reaction is postulated to form $Ru_3(CO)_{11}SbPh_3$. Interestingly, this reaction conducted at room temperature has resulted in the breaking of Ru-Ru bond and formed the open triruthenium cluster. It shows the Sb-C bond cleavages in $SbPh_3$ and a phenyl group insertion into the carbonyl ligand [65].

The reported clusters and the selected bond lengths of $Ru_3(CO)_{12-n}(L)_n$ (n =1, 2, 3) are shown in Table 2.1, Table 2.2 and Table 2.3. The Ru-Ru bond lengths in $Ru_3(CO)_{11}L$ complexes showed the longest bond in the Ru-Ru bond that is *cis* to As/P ligands as a result of steric interactions between the Group 15 ligand and the CO and the CO group *cis* to it on the adjacent Ru atom [60]. Indeed, the Ru-P/As distances increase with increasing cone angle. As compared with $Ru_3(CO)_{10}L_2$ complexes, no pronounced lengthening of the Ru-Ru bond *cis* to the Group 15

ligands and the differences among the three Ru atom separations are not large [61]. For $Ru_3(CO)_9L_3$ complexes, the bond length of Ru-Ru separations are almost similar [62]. However, until recently, no reports on crystal structure of disubstituted and trisubstitued triruthenium substitution with monodentate arsine ligand and very few structure for $Ru_3(CO)_8(L)_4$ complexes have been reported.

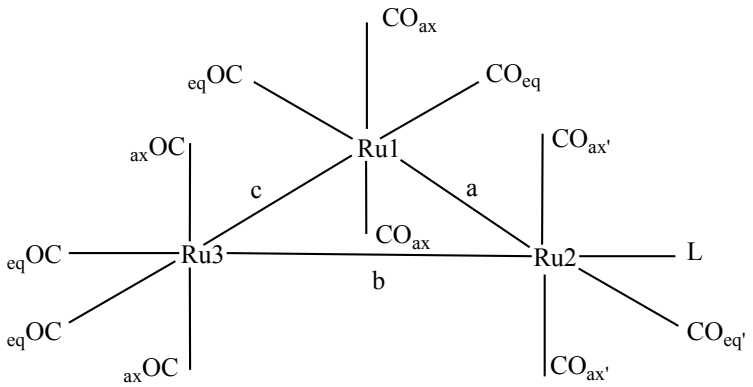

Figure 2.2 Structure diagrams of monosubstituted complexes by monodentate ligand

Table 2.1 Bond lengths (Å) in $Ru_3(CO)_{11}(L)$ complexes

L	Ru-Ru			Ru-L	Ru-C				Reference
	a	b	c		ax'[e]	eq'	ax[f]	eq[f]	
PPh_3	2.907(3)	2.876(3)	2.875(3)	2.380(6)	1.920	1.860(3)	1.940	1.895	[30]
$P(C_6H_4F\text{-}p)_3$	2.876(4)	2.849(4)	2.842(4)	2.349(11)	1.931	1.889(3)	1.942	1.924	[53]
$P(C_6H_4F\text{-}m)_3$	2.905(3)	2.867(3)	2.858(4)	2.364(7)	1.935	1.887(3)	1.942	1.914	[53]
PCy_3[d]	2.902(2)	2.877(2)	2.859(2)	2.424(3)	1.938	1.896(1)	1.934	1.924	[54]
	2.920(2)	2.875(2)	2.874(2)	2.419(3)	1.921	1.871(1)	1.949	1.905	
$PFcPh_2$	2.900(6)	2.864(6)	2.856(7)	2.369(1)	1.925	1.889(5)	1.931	1.918	[66]
$AsPh_3$	2.895(1)	2.850(1)	2.859(1)	2.464(1)	1.933	1.887(4)	1.937	1.907	[60]

[d] Values of two independent molecules. [e] Average of two. [f] Average of four. [g] Read $CO_{eq'}$ as L

Table 2.1 (Continued)

L	Ru-Ru			Ru-L	Ru-C				Reference
	a	b	c		ax'[e]	eq'	ax[f]	eq[f]	
$PPh(OMe)_2$	2.872(1)	2.846(1)	2.858(1)	2.287(1)	1.933	1.888(4)	1.943	1.909	[60]
$P(OCH_2)_3CEt$[g]	2.829(2)	2.858(1)	2.839(2)	2.238(1)	1.924	1.879(6)	1.941	1.905	[60]
$P(OCH_2CF_3)_3$	2.862(1)	2.859(1)	2.846(1)	2.254(1)	1.931	1.911(5)	1.943	1.904	[60]
$P(C_6H_4Me\text{-}p)_3$	2.884(2)	2.840(2)	2.844(2)	2.346(6)	1.941	1.890(2)	1.945	1.926	[29]
$PPh_2(C_6H_4Me\text{-}p)$	2.897(3)	2.852(3)	2.848(3)	2.348(7)	1.940	1.891(3)	1.941	1.925	[29]
$PPh_2(C_6F_5)$	2.887(4)	2.852(4)	2.853(4)	2.343(10)	1.943	1.883(5)	1.947	1.922	[29]
$P(C_6H_4Cl\text{-}p)_3$	2.889(14)	2.837(14)	2.833(15)	2.346(3)	1.941	1.897(15)	1.942	1.928	[29]
$P(3,5\text{-}CF_3\text{-}C_6H_3)_3$	2.888(2)	2.833(2)	2.819(2)	2.334(6)	1.939	1.904(2)	1.949	1.931	[29]
$PPh_2(C_9H_8N)$	2.901(7)	2.863(7)	2.865(7)	2.367(9)	1.935	1.892(4)	1.946	1.922	[67]
$PPh(C_9H_8N)_2$	2.869(7)	2.845(4)	2.841(7)	2.359(9)	1.942	1.885(3)	1.951	1.921	[67]
$PPh(C_{17}H_{12}N_2)$	2.889(5)	2.860(5)	2.864(5)	2.343(1)	1.930	1.895(4)	1.941	1.919	[67]
$P(EtO)_3$[g]	2.835(2)	2.861(2)	2.844(2)	2.281(6)	1.939	1.896(2)	1.942	1.923	[68]
$P(OMe)_3$[g]	2.869(3)	2.888(3)	2.874(3)	2.275(7)	1.926	1.896(3)	1.937	1.919	[69]
$P(Et)_3$[g]	2.865(2)	2.908(2)	2.880(3)	2.349(5)	1.929	1.878(3)	1.942	1.913	[69]
$P(OPh)_3$	2.852(1)	2.844(1)	2.848(1)	2.256(2)	1.941	1.912(6)	1.957	1.909	[70]
$P(OCH_2CH_2Cl)_3$	2.861(4)	2.843(4)	2.862(4)	2.261(7)	1.946	1.905(3)	1.945	1.926	[71]
$P(C_6H_4Cl\text{-}m)_3$	2.860(3)	2.900(4)	2.861(4)	2.359(8)	1.939	1.882(3)	1.938	1.922	[72]
$As(C_6H_4Me\text{-}p)_3$	2.875(5)	2.843(5)	2.869(5)	2.463(5)	1.928	1.893(5)	1.932	1.919	[73]
$As(C_6H_4SCH_3)_3$[g]	2.836(3)	2.895(3)	2.858(3)	2.452(3)	1.934	1.890(3)	1.942	1.921	[74]

[d] Values of two independent molecules. [e] Average of two. [f] Average of four. [g] Read $CO_{eq'}$ as L

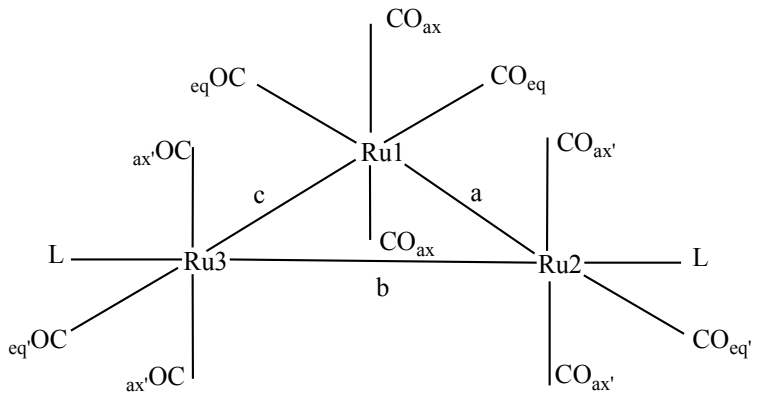

Figure 2.3 Structure diagrams of disubstituted complexes by monodentate ligand

Table 2.2 Bond lengths (Å) in $Ru_3(CO)_{10}(L)_2$ complexes

L	Ru-Ru			Ru-L	Ru-CO				Reference
	a	b	c		ax[e]	eq[e]	ax'[f]	eq'[e]	
$P(C_6H_4F\text{-}p)_3$[d]	2.861(8)	2.872(6)	2.861(8)	2.367	1.969	1.923	1.943	1.881	[53]
	2.871(8)	2.848(6)	2.871(8)	2.358	1.912	1.968	1.942	1.865	[53]
$P(OMe)_3$	2.859(1)	2.845(1)	2.845(1)	2.298	1.930	1.890	1.940	1.920	[54]
PPh_3[d]	2.842(4)	2.846(3)	2.838(4)	2.357	1.940	1.860	1.840	1.870	[61]
	2.873(3)	2.893(3)	2.881(3)	2.380	1.910	1.870	1.890	1.890	[61]
$PPh(OMe)_2$	2.865(1)	2.860(1)	2.868(1)	2.297	1.929	1.888	1.929	1.907	[61]
$P(OCH_2CF_3)_3$	2.847(2)	2.831(2)	2.861(2)	2.250	1.910	1.870	1.960	1.890	[61]
$P(Et)_3$	2.868(2)	2.855(2)	2.863(2)	2.351	1.972	1.909	1.952	1.889	[75]
$P(C_6H_4Cl\text{-}m)_3$	2.865(3)	2.852(3)	2.863(3)	2.343	1.951	1.914	1.938	1.887	[76]
$P(Me_2(nap))$	2.881(4)	2.843(3)	2.869(3)	2.345	1.937	1.917	1.931	1.883	[77]
$P(C_4H_3S)_3$	2.945(13)	2.880(12)	3.001(12)	2.352	1.955	1.934	1.925	1.969	[78]

[d] Values of two independent molecule. [e] Average of two. [f] Average of four.

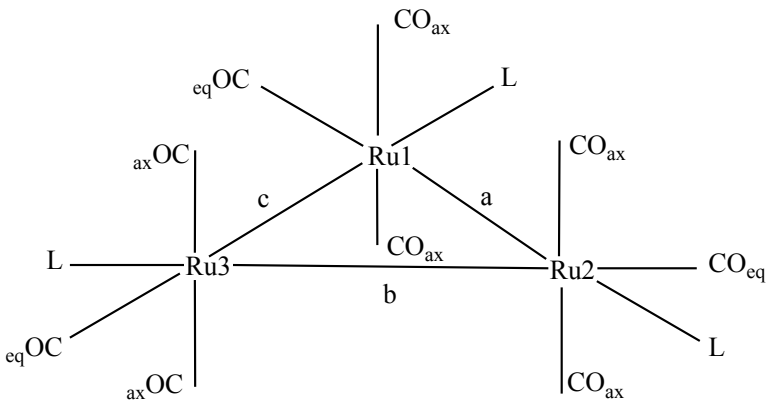

Figure 2.4 Structure diagrams of trisubstituted complexes by monodentate ligand

Table 2.3 Bond lengths (Å) in $Ru_3(CO)_9(L)_3$ complexes

L	Ru-Ru			Ru-L	Ru-C		Reference
	a	b	c		ax[f]	eq[g]	
$P(C_6H_4F\text{-}m)_3$	2.885(3)	2.886(3)	2.877(3)	2.337	1.934	1.890	[53]
$P(Me)_3$	2.860(1)	2.862(2)	2.854(1)	2.331	1.919	1.868	[54]
$PPh(Me)_2$	2.864(1)	2.851(1)	2.860(1)	2.334	1.916	1.871	[61]
$PMe_2(CH_2Ph)$	2.860(2)	2.860(2)	2.860(2)	2.314	1.930	1.880	[61]
$PPh(OMe)_2$[e]	2.870(1)	2.900(1)	2.887(2)	2.284	1.922	1.909	[61]
	2.894(1)	2.887(1)	2.876(2)	2.279	1.927	1.887	[61]
	2.876(1)	2.884(1)	2.882(1)	2.278	1.924	1.878	[61]
	2.874(2)	2.882(4)	2.885(1)	2.299	1.934	1.915	[61]
$P(OEt)_3$	2.852(2)	2.863(1)	2.851(1)	2.292	1.950	1.900	[61]
$P(OCH_2CF_3)_3$	2.866(2)	2.857(2)	2.852(2)	2.246	1.930	1.850	[61]
$AsMe_2Ph$[d]	2.846(1)	2.851(1)	2.838(1)	2.444	1.919	1.862	[62]
	2.848(1)	2.846(1)	2.838(1)	2.446	1.925	1.870	[62]
$(PTA)_3$	2.878(8)	2.873(8)	2.870(7)	2.297	1.924	1.884	[79]
$PPh_2(CH_2)_3Ph$	2.868(13)	2.868(15)	2.868(13)	2.332	1.925	1.878	[80]
PPh_3	2.862(6)	2.868(7)	2.889(7)	2.340	1.934	1.879	[81]
PCy_3	2.939(8)	2.939(8)	2.939(8)	2.414	1.929	1.875	[82]
$PPh_2(C_6H_4CCF)_3$	2.885(2)	2.884(2)	2.888(2)	2.351	1.921	1.897	[83]
$P(OMe)_3$	2.844(10)	2.849(11)	2.869(10)	2.280	1.927	1.889	[84]

[d] Values of two independent molecules. [e] Values of four independent molecules.
[f] Average of six. [g] Average of three.

2.2 Substitution chemistry of triruthenium cluster complexes with bidentate ligands

The chemical reactions of bidentate ligands with $Ru_3(CO)_{12}$ had started since 1970 and has been explored by Cullen and Harbourne. They reported the reactions between $Ru_3(CO)_{12}$ with the fluorocarbon-bridged ligands, ffars, ffos and $f_6$fos, respectively [45]. The similarity of both $Ru_3(CO)_8(ffars)_2$ and $Ru_3(CO)_8(ffos)_2$ infrared spectra within the carbonyl stretching region indicates that they are isostructural. Since the initial studies, the substitution chemistry and subsequent reactivities and reaction mechanisms of the type $Ru_3(LL)(CO)_{10}$ and $Ru_3(LL)_2(CO)_8$ have been studied extensively.

Generally, the possible compounds formed from the reaction of bidentate ligands between $Ru_3(CO)_{12}$ are shown in Figure 2.5. The bidentate ligands have potential to bind to a metal centre by chelating a single ruthenium atom within the cluster, by bridging a cluster edge and binding two ruthenium atoms, or by acting as monodentate ligand with one freely dangling atom. In 1977, Cotton and Hanson first reported the synthesis of $Ru_3(CO)_{10}$(dppm) from the reaction between $Ru_3(CO)_{12}$ and dppm refluxed at 50˚C for 36 hours [85]. No yield and crystal structure was reported from this reaction but the $Ru_3(CO)_{10}$(dppm) complex was confirmed by the characteristic pattern of carbonyl stretching frequencies for disubstituted complexes. Later, Bruce and co-workers reported the synthesis of $Ru_3(CO)_{10}$(dppm) at 91% yield by using sodium benzophenone ketyl radical [86].

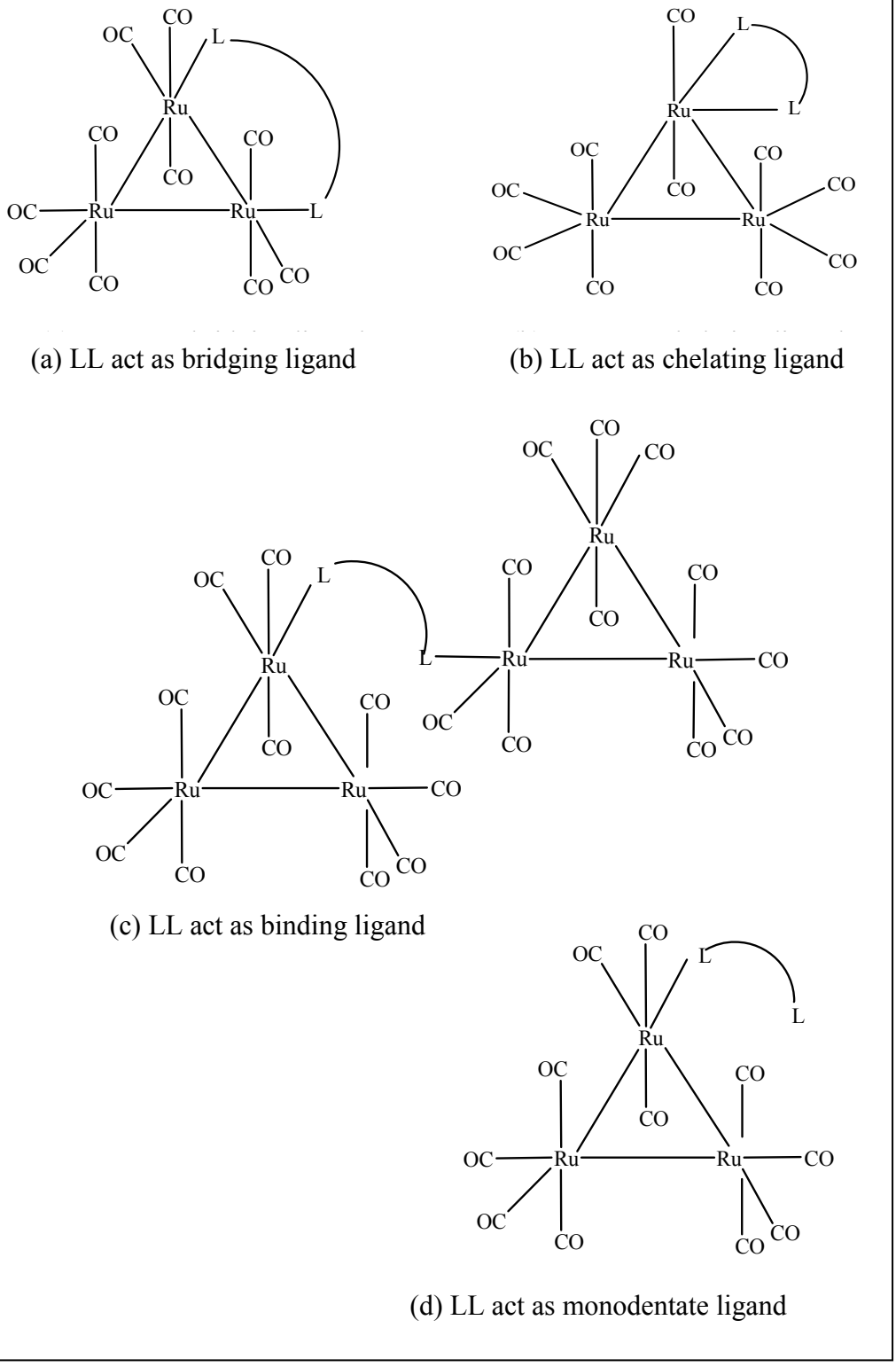

Figure 2.5 General reaction structures of bidentate ligand with triruthenium cluster

The crystal structure of $Ru_3(CO)_{10}$(dppm) were reported by Coleman and co-workers resulting from the reaction of excess $Fe_2(CO)_9$ to the ruthenium (II) dimer [{$RuCl_2$(cymene)}$_2$(μ-η^1,η^1-dppm)] which afforded $Ru_3(CO)_{10}$(dppm) in 15% yield and the mixed-metal analogue [$FeRu_2(CO)_{10}$(μ-dppm)] in 37% yield [35]. The interesting abnormality found in this structure was the strain in the five-membered chelate rings, as dppm has a greater tendency to bridge across a metal-metal bond than chelate to a single metal atom [41]. Indeed, the reaction of $Ru_3(CO)_{12}$ with dppm was also afforded $Ru_3(CO)_8$(μ-dppm)$_2$ by heating $Ru_3(CO)_{12}$ and dppm in 1:2 ratio in xylene between 80 and 85˚C [87] while $Ru_3(CO)_6$(μ-dppm)$_3$ was prepared from the reduction of ruthenium (III) acetate by $NaBH_4$ in the presence of excess dppm and CO [88].

The other triruthenium cluster of the type $Ru_3(CO)_{10}$(LL) where LL= bidentate ligand that consists of one carbon backbone is $Ru_3(CO)_{10}$(dpam). The longest Ru-Ru bond that was found in this structure was bridged by bidentate ligand as compared to related bond in $Ru_3(CO)_{10}$(dppm) which have similar one carbon backbone. Shawkataly and co-workers suggested that the significant shortening of unbridged Ru-Ru bond probably arising from dissimilarity in the σ-donor character of the diarsine relative to the CO group [89].

The preparation of dppe derivatives of $Ru_3(CO)_{12}$ was reported in 1982 by using different ratio of quantity of $Ru_3(CO)_{12}$ and dppe in the presence of sodium benzophenone ketyl radical anion afforded $Ru_3(CO)_8$(dppe)$_2$, $Ru_3(CO)_{10}$(dppe), $Ru_3(CO)_{11}$(dppe) and [$Ru_3(CO)_{11}$]$_2$(dppe). All compounds were characterized and only the crystal structure of $Ru_3(CO)_{10}$(dppe) was reported [36]. In 1998, crystal structure of [$Ru_3(CO)_{11}$]$_2$(dppe) was reported and showed no direct interactions

between two triruthenium molecule; since the clusters are offset at opposite ends of molecules [90]. Similar observation was also seen in $[Ru_3(CO)_{11}]_2$dppbz [90].

In addition, the extensive study with regard to variations of substituents at phosphorus atom and nature of carbon backbone of diphosphine ligands have resulted in the novel complexes of disubstituted complexes. For example, the bulky diphosphine ligands bis(dicyclohexylphosphino)methane (dcpm) and bis(perfluoro-diphenylphosphino)ethane (F-dppe) are able to coordinate with $Ru_3(CO)_{12}$ to form $Ru_3(CO)_{10}$(dcpm) and $Ru_3(CO)_{10}$(F-dppe). With an excess of dcpm and F-dppe, the thermal reaction of $Ru_3(CO)_{12}$ gives bis(diphosphine) clusters $Ru_3(CO)_8(dcpm)_2$ and $Ru_3(CO)_8(F\text{-}dppe)_2$. The unique findings through this study found that the complex $Ru_3(CO)_8(F\text{-}dppe)_2$ consists of different structure with an unprecedented arrangement of the two diphosphine ligands. This shows that one of the F-dppe ligand is μ_2-η^2 coordinated to two different Ru atoms, while the other one is μ_1-η^2 coordinated to the third Ru atom. Generally, complex that consists of the two diphosphine ligands is in normal μ_2-η^2 coordination mode as observed for $Ru_3(CO)_8(dppm)_2$ [91]. On the other hand, the strong tendency of bidentate diphoshine and diarsine to adopt an μ_2-η^2 coordination mode also has been previously noticed in the crystal structure of $Ru_3(CO)_8$(dppm)(dpam) [92].

Another remarkable ligand due to the various coordination modes that it can adopt to balance the sterics of the existing environtment is dppf. $Ru_3(CO)_{12}$ typically reacts with sodium benzophenone ketyl radical anion afforded a number of products and they are difficult to be isolated by chromatography and generally unstable in solution. Only one product was air stable and recognized as $Ru_3(CO)_{10}$(dppf) [66]. By refluxing $Ru_3(CO)_{12}$ and dppf in cyclohexane afforded $Ru_3(CO)_8(dppf)_2$ [66].

Indeed, the synthesis and crystal structure of $[Ru_3(CO)_{11}]_2$dppf were also reported [31].

Recently, the triruthenium cluster containing the hybrid ligand, $Ru_3(CO)_{10}$(P,P'-mapm) was prepared between $Ru_3(CO)_{12}$ and mapm in THF for 10 minutes at ambient temperature [93]. The related complex $Ru_3(CO)_{10}$(dppa) has been prepared from $Ru_3(CO)_{12}$ with dppa in the presence of a catalytic amount of benzophenone ketyl radical anion which has been crystallographically characterized [94]. Indeed, by using the same method, a range of triruthenium complexes containing axially chiral diphosphazane ligands have been reported [95]. Another hybrid bidentate ligand coordinate with triruthenium cluster is arphos ligand which afforded $Ru_3(CO)_{10}$(arphos) [96]. The crystal structure of this complex is almost similar to $Ru_3(CO)_{10}$(dppe) [36].

The coordination of Group 15 bidentate ligands in all reported triruthenium cluster occupy equatorial position as a result of steric effect leads to the variation of Ru-Ru bond lengths. The reported crystal structure of $Ru_3(CO)_{10}$(LL) and selected bond lengths are reported in Table 2.4. Some of Ru-Ru bond lengths that are bridged by bidentate ligand possess the longest Ru-Ru bond as compared to other Ru-Ru bonds. The nature of substituents at phosphorus atom and number of carbon backbone of diphosphine ligands affect the Ru-Ru and Ru-CO bond lengths. For example, in the case of the series of $Os_3(CO)_{10}(Ph_2P(CH_2)_nPPh_2)$ (n=1,2,4,5), clearly shows number of carbon backbone has an effect in the Os-Os bond that are bridged by these bidentate ligand [38, 97-98]. The Os-Os bond, bridged by the bidentate ligand is the longest Os-Os bond in comparison to others. In these bidentate ligands, the two phosphorus atoms are connected by saturated carbon backbone. This phenomenon is also related to the bite angle of the bidentate ligand.